

# Heteroleptic Ruthenium(II) 2,2'-Bipyridine Complexes Incorporating Bipyrazolate and 2-Pyridyl Pyrazolate Ancillaries

M. L. Cheng<sup>a</sup>, L. H. Tang<sup>a</sup>, Z. Qian<sup>a</sup>, A. Q. Jia<sup>a</sup>, and Q. F. Zhang<sup>a, \*</sup>

<sup>a</sup> Institute of Molecular Engineering and Applied Chemistry, Anhui University of Technology, Ma'anshan, Anhui, 243002 P.R. China

\*e-mail: zhangqf@ahut.edu.cn

Received June 23, 2020; revised June 28, 2020; accepted July 22, 2020

**Abstract**—Treatment of 5,5'-di(trifluoromethyl)-3,3'-bipyrazole (BipzH<sub>2</sub>) with *cis*-[RuCl<sub>2</sub>(Bipy)<sub>2</sub>]<sup>2+</sup>·2H<sub>2</sub>O (Bipy = 2,2'-bipyridine) or *cis*-[RuCl<sub>2</sub>(Dmbipy)<sub>2</sub>]<sup>2+</sup>·2H<sub>2</sub>O (Dmbipy = 4,4'-dimethyl-2,2'-bipyridine) afforded two charge-neutral ruthenium(II) complexes [Ru(Bipz)(Bipy)<sub>2</sub>] (**I**) and [Ru(Bipz)(Dmbipy)<sub>2</sub>] (**II**), respectively. Reactions of 3-trifluoromethyl-5-(2-pyridyl)pyrazole (PypzH) and *cis*-[RuCl<sub>2</sub>(Bipy)<sub>2</sub>]<sup>2+</sup>·2H<sub>2</sub>O or *cis*-[RuCl<sub>2</sub>(Dmbipy)<sub>2</sub>]<sup>2+</sup>·2H<sub>2</sub>O in the presence of NH<sub>4</sub>PF<sub>6</sub> produced two cationic ruthenium(II) complexes [Ru(Pypz)(Bipy)<sub>2</sub>](PF<sub>6</sub>) (**III**) and [Ru(Pypz)(Dmbipy)<sub>2</sub>](PF<sub>6</sub>) (**IV**), respectively. Four complexes were spectroscopically characterized by FTIR, UV-Vis and luminescence. The structures of **I**·H<sub>2</sub>O, **III**·H<sub>2</sub>O and **IV** have been also determined by single-crystal X-ray diffraction (CIF files CCDC nos. 1935282–1935284, respectively).

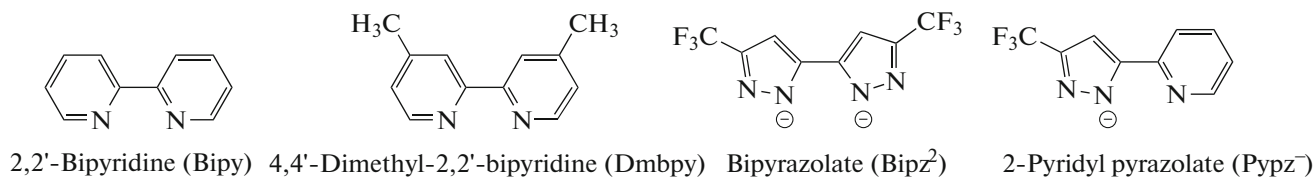
**Keywords:** heteroleptic ruthenium complex, 2,2'-bipyridine, pyrazolate, synthesis, crystal structure

**DOI:** 10.1134/S1070328421050018

## INTRODUCTION

It is well known that ruthenium(II) complexes of the [Ru(Bipy)<sub>3</sub>]<sup>2+</sup> (Bipy = 2,2'-bipyridine) family are especially interesting due to systematic modifications in the bulky backbone and their possible applications in energy conversion and photo induced electron transfer processes [1–3]. In comparison to the poly-pyridyl systems, study on ruthenium-Bipy complexes with the other *N*-containing heterocycles, e.g., imidazole, pyrazole, pyrazine is limited [4–6]. Actually, coordination of such heterocycles to ruthenium center could alter the electron transfer and optical properties of the afforded ruthenium complexes due to the different electron donor/acceptor properties of the coordinating nitrogen atoms [7]. In the past decade, the dianionic chelate ligand Bipz (BipzH<sub>2</sub> = 5,5'-di(trifluoromethyl)-3,3'-bipyrazole) have been employed to synthesize ruthenium(II), osmium(II), platinum(II) and iridium(III) complexes with unique properties [8–11]. For examples, ruthenium(II) complexes incorporating dianionic bipyrazolate ancillaries are suited for high performance dye sensitized solar cells (DSCs) [11]; iridium(III) complexes with dianionic Bipz chelate can serve as decent dopant emitters in organic light-emitting diode (OLED) devices [12].

On the other hand, the strong  $\sigma$ -donor property of the pyrazolate unit, together with the good  $\pi$ -accepting ability of the second pyridyl fragment, provides a synergism of the electron delocalization over the whole ligand  $\pi$  conjugation as well as the metal  $d\pi$  orbitals [13]. It has been noted that ruthenium(II)-terpyridine complexes bearing pyridine pyrazolate chelates have shown their superior dye-sensitized solar cell performance [14]. Moreover, it has showed in [15] substituents of carboxy groups on Bipy unit is detrimental to the fabrication of very high efficiency DSC devices. Recently, we have reported the syntheses and phosphorescent properties of several heteroleptic ruthenium(II)/(III) polypyridine complexes with a series of substituted 2,2'-bipyridine ligands, Schiff base *N,O*-ligands and *N,C*-phenylphthalazine ligands [16–18]. In this paper, we report the synthesis, structure and electronic properties of four heteroleptic ruthenium(II)-Bipy/Dmbipy (Bipy = 2,2'-bipyridine; Dmbipy = 4,4'-dimethyl-2,2'-bipyridine) complexes: [Ru(Bipz)(Bipy)<sub>2</sub>]<sup>2+</sup>·H<sub>2</sub>O (**I**·H<sub>2</sub>O), [Ru(Bipz)(Dmbipy)<sub>2</sub>] (**II**), [Ru(Pypz)(Bipy)<sub>2</sub>](PF<sub>6</sub>) (**III**·H<sub>2</sub>O) and [Ru(Pypz)(Dmbipy)<sub>2</sub>](PF<sub>6</sub>) (**IV**) with bipyrazolate (Bipz<sup>2-</sup>) and 2-pyridyl pyrazolate (Pypz<sup>-</sup>). Chelating ligands with varying electronic character are below:



## EXPERIMENTAL

**Materials and methods.** All synthetic manipulations were carried out under dry nitrogen by standard Schlenk techniques.  $\text{RuCl}_3 \cdot 3\text{H}_2\text{O}$  was used as purchased from Pressure Chemical Co. Ltd. *cis*- $[\text{RuCl}_2(\text{Bipy})_2] \cdot 2\text{H}_2\text{O}$  [19], *cis*- $[\text{RuCl}_2(\text{Dmbipy})_2] \cdot 2\text{H}_2\text{O}$  [20], BipzH<sub>2</sub> [21] and 3-trifluoromethyl-5-(2-pyridyl)pyrazole (PypzH) [11] were prepared according to the literature methods. Infrared spectra were recorded in KBr pellets on a Perkin-Elmer 16 PC FTIR spectrophotometer. NMR spectra were recorded on a Bruker ALX 400 spectrometer operating at 400 MHz for <sup>1</sup>H, 376 MHz for <sup>19</sup>F, and 162 MHz for <sup>31</sup>P. Electronic absorption spectra were obtained on a Shimadzu UV-3000 spectrophotometer. Photoluminescence (PL) spectra were measured with a Shimadzu RF-5301PC fluorescence spectrophotometer. Positive-ion ESI mass spectra were recorded on a Perkin Elmer Sciex API 365 mass spectrometer. Elemental analyses were carried out using a Perkin-Elmer 2400 CHN analyzer.

**Synthesis of  $[\text{Ru}(\text{Bipz})(\text{Bipy})_2] \cdot \text{H}_2\text{O}$  (I·H<sub>2</sub>O).** A mixture of BipzH<sub>2</sub> (27 mg, 0.10 mmol) and *cis*- $[\text{Ru}(\text{Bipy})_2\text{Cl}_2] \cdot 2\text{H}_2\text{O}$  (52 mg, 0.10 mmol) was stirred in 20 mL ethanol–H<sub>2</sub>O (v : v = 1 : 1) at 85°C for 3 h, during which the color of the solution turned to reddish brown. After removing the solvent, the solid product was washed with diethyl ether (5 mL × 3) to give the desired product. Recrystallization from CH<sub>2</sub>Cl<sub>2</sub>–*n*-hexane (v : v = 1 : 3) gave dark red block crystals of I·H<sub>2</sub>O in a week. The yield was 33 mg (49% based on Ru).

For C<sub>28</sub>H<sub>18</sub>N<sub>8</sub>F<sub>6</sub>Ru·H<sub>2</sub>O

Anal. calcd., %	C, 48.07	H, 2.88	N, 16.02
Found, %	C, 48.03	H, 2.86	N, 16.05

IR (KBr; v, cm<sup>-1</sup>): v(C=C) 1617, v(N–N) 1384, v(C–F) 1129. <sup>1</sup>H NMR (D<sub>6</sub>[DMSO]; δ, ppm): 8.64 (d., J = 7.8 Hz, 2H), 8.57 (d., J = 7.7 Hz, 2H), 7.99 (dt., J = 16.1, 7.6 Hz, 8H), 7.58–7.49 (m., 2H), 7.38–7.29 (m., 2H), 7.14–6.98 (m., 2H). <sup>19</sup>F NMR (D<sub>6</sub>[DMSO]; δ, ppm): -57.17 (s., CF<sub>3</sub>), -59.08 (s., CF<sub>3</sub>). MS (FAB): *m/z* 681 [M]<sup>+</sup>.

**Synthesis of  $[\text{Ru}(\text{Bipz})(\text{Dmbipy})_2]$  (II).** A mixture of BipzH<sub>2</sub> (27 mg, 0.10 mmol) and *cis*- $[\text{Ru}(\text{Dmbipy})_2\text{Cl}_2] \cdot 2\text{H}_2\text{O}$  (55 mg, 0.10 mmol) was stirred in 25 mL ethanol–H<sub>2</sub>O (v : v = 1 : 1) at 85°C for 2 h, during which the color of the solution turned

to orange reddish. After removing the solvent, the solid product was washed with diethyl ether (5 mL × 3) to give the desired product. Recrystallization from CH<sub>2</sub>Cl<sub>2</sub>–*n*-hexane (v : v = 1 : 3) gave dark red block crystals of II in five days. The yield was 34 mg (46% based on Ru).

For C<sub>32</sub>H<sub>26</sub>N<sub>8</sub>F<sub>6</sub>Ru

Anal. calcd., %	C, 52.10	H, 3.55	N, 15.19
Found, %	C, 52.07	H, 3.56	N, 15.21

IR (KBr; v, cm<sup>-1</sup>): 1616 v(C=C), 1384 v(N–N), 1126 v(C–F). <sup>1</sup>H NMR (D<sub>6</sub>[DMSO]; δ, ppm): 8.62 (d., J = 7.8 Hz, 2H), 8.57 (d., J = 7.7 Hz, 2H), 7.96 (dt., J = 16.1, 7.6 Hz, 6H), 7.58–7.49 (m., 2H), 7.21–6.96 (m., 2H), 2.62 (s., 3H, CH<sub>3</sub>), 2.56 (s., 3H, CH<sub>3</sub>), 2.46 (s., 3H, CH<sub>3</sub>) 2.41 (s., 3H, CH<sub>3</sub>). <sup>19</sup>F NMR (D<sub>6</sub>[DMSO]; δ, ppm): -57.01 (s., CF<sub>3</sub>), -60.78 (s., CF<sub>3</sub>). MS (FAB): *m/z* 738 [M]<sup>+</sup>.

**Synthesis of  $[\text{Ru}(\text{Pypz})(\text{Bipy})_2](\text{PF}_6)$  (III·H<sub>2</sub>O).** A mixture of PypzH (21 mg, 0.10 mmol) and *cis*- $[\text{Ru}(\text{Bipy})_2\text{Cl}_2] \cdot 2\text{H}_2\text{O}$  (52 mg, 0.10 mmol) was stirred in 20 mL ethanol–H<sub>2</sub>O (v : v = 1 : 1) at 80°C for 2.5 h, during which the color of the solution turned to dark red. After filtering the solution, an excess of an ammonium hexafluorophosphate (0.30 mmol, 49 mg) solution in ethanol (5 mL) was added, and the mixture was further stirred at room temperature for 15 min. The suspension was filtered and the precipitate was washed with diethyl ether (7 mL × 3) to give the desired orange-yellow product. Recrystallization of the crude product from acetone–*n*-hexane (v : v = 1 : 3) gave orange-red block crystals of III·H<sub>2</sub>O in a week. The yield was 39 mg (50% based on Ru).

IR (KBr; v, cm<sup>-1</sup>): 1620 v(C=C), 1385 v(N–N), 1128 v(C–F). <sup>1</sup>H NMR (D<sub>6</sub>[DMSO]; δ, ppm): 8.41 (m., 3H), 8.27 (m., 3H), 7.96–7.80 (m., 5H), 7.74 (m., 5H), 7.48 (m., 2H), 7.42–7.34 (m., 2H), 7.04 (s., 1H); <sup>19</sup>F NMR (D<sub>6</sub>[DMSO]; δ, ppm): -58.14 (s., CF<sub>3</sub>), -70.14 (d., J = 711 Hz, PF<sub>6</sub>). <sup>31</sup>P NMR (D<sub>6</sub>[DMSO]; δ, ppm): -144.22 (m., PF<sub>6</sub>). MS (FAB): *m/z* 626 [M – PF<sub>6</sub>]<sup>+</sup>.

For C<sub>29</sub>H<sub>21</sub>N<sub>7</sub>F<sub>9</sub>PRu·H<sub>2</sub>O

Anal. calcd., %	C, 44.17	H, 2.94	N, 12.43
Found, %	C, 44.14	H, 2.96	N, 12.45

**Synthesis of  $[\text{Ru}(\text{Pypz})(\text{Dmbipy})_2](\text{PF}_6)$  (IV).** A mixture of PypzH (21 mg, 0.10 mmol) and *cis*- $[\text{Ru}(\text{Dmbipy})_2\text{Cl}_2]\cdot 2\text{H}_2\text{O}$  (58 mg, 0.10 mmol) was stirred in 20 mL ethanol– $\text{H}_2\text{O}$  ( $v:v=1:1$ ) at 80°C for 3 h, during which the color of the solution turned red. After filtering the solution, an excess of an ammonium hexafluorophosphate (0.30 mmol, 49 mg) solution in ethanol (5 mL) was added, and the mixture was further stirred at room temperature for 15 min. The suspension was filtered and the precipitate was washed with diethyl ether ( $7\text{ mL} \times 3$ ) to give the desired red product. Recrystallization with dichloromethane–*n*-hexane ( $v:v=1:4$ ) gave red block crystals of **IV** in six days. The yield was 39 mg (48% based on Ru).

8.22 (m., 2H), 8.02 (m., 2H), 7.72 (m., 2H), 7.65 (d.,  $J=5.7$  Hz, 1H), 7.58–7.51 (m., 2H), 7.47 (d.,  $J=5.5$  Hz, 2H), 7.24 (s., 1H), 7.13 (m., 2H), 7.05 (m., 2H), 7.00 (s., 1H), 2.57 (s  $\times 2$ , 6H,  $\text{CH}_3$ ), 2.48 (s., 3H,  $\text{CH}_3$ ) 2.36 (s., 3H,  $\text{CH}_3$ );  $^{19}\text{F}$  NMR ( $\text{D}_6[\text{DMSO}]$ ;  $\delta$ , ppm): –57.99 (s.,  $\text{CF}_3$ ), –70.20 (d.,  $J=680$  Hz,  $\text{PF}_6$ ).  $^{31}\text{P}$  NMR ( $\text{D}_6[\text{DMSO}]$ ;  $\delta$ , ppm): –144.21 (m.,  $\text{PF}_6$ ). MS (FAB):  $m/z$  682 [M] $^+$ .

For  $\text{C}_{33}\text{H}_{29}\text{N}_7\text{F}_9\text{PRu}$

Anal. calcd., % C, 47.88 H, 3.53 N, 11.85  
Found, % C, 47.84 H, 3.55 N, 11.88

**X-ray crystallography.** Intensity data were collected on a Bruker SMART APEX 2000 CCD diffractometer using graphite-monochromated  $\text{MoK}_\alpha$  radiation ( $\lambda=0.71073$  Å) at 296(2) K. The collected frames were

processed with the software SAINT [22]. The data was corrected for absorption using the program SADABS [23]. Structures were solved by the direct methods and refined by full-matrix least-squares on  $F^2$  using the SHELXTL software package [24]. All non-hydrogen atoms were refined anisotropically. The positions of all hydrogen atoms were generated geometrically ( $\text{C}_{\text{sp}3}-\text{H}=0.97$  and  $\text{C}_{\text{sp}2}-\text{H}=0.93$  Å), assigned isotropic thermal parameters, and allowed to ride on their respective parent carbon atoms before the final cycle of least-squares refinement. A summary of crystallographic data and experimental details for **I**· $\text{H}_2\text{O}$ , **III**· $\text{H}_2\text{O}$ , and **IV** are summarized in Table 1. Selected bond lengths and bond angles are given in the figure captions (Figs. 1–3). The hydrogen-bond characteristics and geometric parameters for the three complexes are listed in Table 2.

Supplementary material for structures has been deposited with the Cambridge Crystallographic Data Centre (CCDC nos. 1935282 (**I**· $\text{H}_2\text{O}$ ), 1935283 (**III**· $\text{H}_2\text{O}$ ), and 1935284 (**IV**); deposit@ccdc.cam.ac.uk or <http://www.ccdc.cam.ac.uk>).

## RESULTS AND DISCUSSION

It is noted that the first ruthenium(II) complexes with two 2,2'-bipyridine-type ligands and Bipz $^{2-}$  ligand have already been reported in [11]. With this research in mind, we tried the syntheses of heteroleptic ruthenium(II)-Bipy/Dmbipy complexes **I**–**IV**, as shown in Scheme 1.

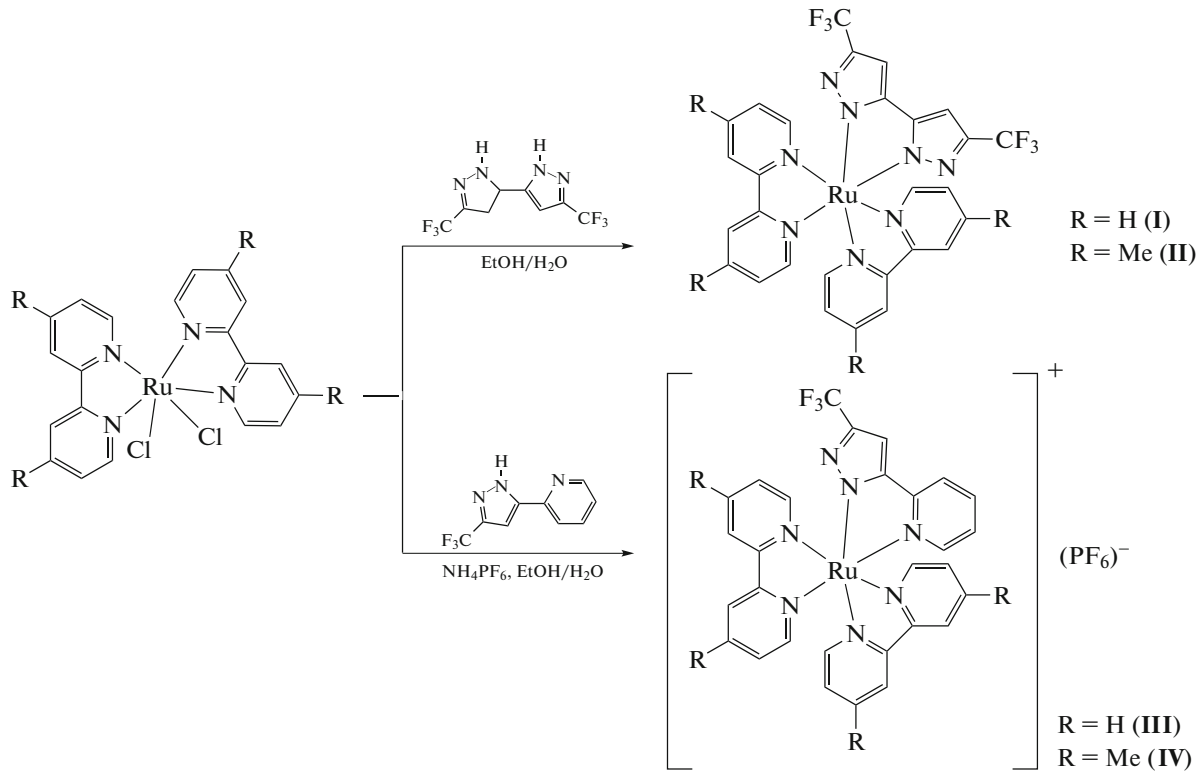


**Table 1.** Crystallographic data and experimental details for **I**·H<sub>2</sub>O, **III**·H<sub>2</sub>O, and **IV**

Parameter	Value		
	<b>I</b> ·H <sub>2</sub> O	<b>III</b> ·H <sub>2</sub> O	<b>IV</b>
Empirical formula	C <sub>28</sub> H <sub>20</sub> N <sub>8</sub> OF <sub>6</sub> Ru	C <sub>29</sub> H <sub>23</sub> N <sub>7</sub> OF <sub>9</sub> PRu	C <sub>33</sub> H <sub>29</sub> N <sub>7</sub> F <sub>9</sub> PRu
Formula weight	699.59	788.58	826.67
Crystal system	Tetragonal	Triclinic	Monoclinic
Space group	<i>P</i> 4 <sub>1</sub> 2 <sub>1</sub> 2	<i>P</i> 1̄	<i>P</i> 2 <sub>1</sub> /n
<i>a</i> , Å	10.455(5)	9.911(3)	11.369(7)
<i>b</i> , Å	10.455(5)	13.468(4)	17.653(10)
<i>c</i> , Å	28.42(3)	13.823(5)	17.823(10)
α, deg	90	78.870(4)	90
β, deg	90	69.862(4)	98.675(11)
γ, deg	90	88.757(5)	90
<i>V</i> , Å <sup>3</sup>	3107(4)	1697.6(10)	3536(3)
<i>Z</i>	4	2	4
ρ <sub>calcd</sub> , g cm <sup>-3</sup>	1.496	1.543	1.553
Temperature, K	296(2)	296(2)	296(2)
<i>F</i> (000)	1400	788	1664
μ(Mo $K_{\alpha}$ ), mm <sup>-1</sup>	0.576	0.593	0.571
Total reflections	9056	8409	22120
Independent reflections	3574	6902	8151
<i>R</i> <sub>int</sub>	0.0805	0.0385	0.1281
<i>R</i> <sub>1</sub> <sup>a</sup> , <i>wR</i> <sub>2</sub> <sup>b</sup> ( <i>I</i> > 2σ( <i>I</i> ))	0.0890, 0.2212	0.0838, 0.2096	0.0750, 0.1638
<i>R</i> <sub>1</sub> , <i>wR</i> <sub>2</sub> (all data)	0.1640, 0.2756	0.1391, 0.2410	0.1871, 0.2276
GOOF <sup>c</sup>	0.966	1.077	0.905
Final max/min diff. peaks, e Å <sup>-3</sup>	0.912/-0.564	0.987/-1.020	0.804/-0.594

<sup>a</sup>  $R_1 = \Sigma |F_o| - |F_c| | / \Sigma |F_o|$ .<sup>b</sup>  $wR_2 = [\Sigma w(|F_o^2| - |F_c^2|)^2 / \Sigma w|F_o^2|^2]^{1/2}$ .<sup>c</sup> GOOF =  $[\Sigma w(|F_o| - |F_c|)^2 / (N_{\text{obs}} - N_{\text{param}})]^{1/2}$ .**Scheme 1.**

Reaction of BipzH<sub>2</sub> and equal equivalent of *cis*-[Ru(Bipy)<sub>2</sub>Cl<sub>2</sub>]·2H<sub>2</sub>O or *cis*-[Ru(Dmbipy)<sub>2</sub>Cl<sub>2</sub>]·2H<sub>2</sub>O in the ethanol–water mixed solvent at reflux afforded the heteroleptic ruthenium(II) complexes [Ru(Bipz)(Bipy)<sub>2</sub>] (**I**) and [Ru(Bipz)(Dmbipy)<sub>2</sub>] (**II**), respectively. The two chloro ligands in *cis*-[Ru(Bipy)<sub>2</sub>Cl<sub>2</sub>]·2H<sub>2</sub>O or *cis*-[Ru(Dmbipy)<sub>2</sub>Cl<sub>2</sub>]·2H<sub>2</sub>O were substituted by dianionic bipyrazolate ligand (Bipz<sup>2-</sup>) to form the neutral heteroleptic polypyridyl ruthenium(II) complexes **I** and **II** in moderate yields. Interaction of PypzH with equivalent of *cis*-[Ru(Bipy)<sub>2</sub>Cl<sub>2</sub>]·2H<sub>2</sub>O or *cis*-[Ru(Dmbipy)<sub>2</sub>Cl<sub>2</sub>]·2H<sub>2</sub>O in the presence of NH<sub>4</sub>PF<sub>6</sub> led to isolation of ruthenium(II) complexes [Ru(Pypz)(Bipy)<sub>2</sub>](PF<sub>6</sub>) (**III**) and [Ru(Pypz)(Dmbipy)<sub>2</sub>](PF<sub>6</sub>) (**IV**), respectively. Obviously, the two chloro ligands in *cis*-

[Ru(Bipy)<sub>2</sub>Cl<sub>2</sub>]·2H<sub>2</sub>O or *cis*-[Ru(Dmbipy)<sub>2</sub>Cl<sub>2</sub>]·2H<sub>2</sub>O were replaced by the monoanionic bidentate 2-pyridyl pyrazolate ligand (Pypz<sup>-</sup>) to obtain the cationic heteroleptic polypyridyl ruthenium(II) complexes **III** and **IV** with PF<sub>6</sub><sup>-</sup> as the counter anion. The <sup>1</sup>H NMR spectra of ruthenium(II) complexes **II** and **IV** display the methyl protons attached to Dmbpy ligands at around 2.5 ppm. The <sup>19</sup>F NMR spectra of ruthenium(II) complexes **I**–**IV** display the signals of –CF<sub>3</sub> groups on pyrazole ring at around –58 ppm, which are similar to those in related complexes (ca. –60 ppm) [12, 15]. Moreover, the <sup>31</sup>P and <sup>19</sup>F NMR spectra of complexes **III** and **IV** exhibit the phosphorous signals at about –144 ppm and fluorine signals at about –70 ppm, which are typical of PF<sub>6</sub><sup>-</sup> anion. All the synthesized

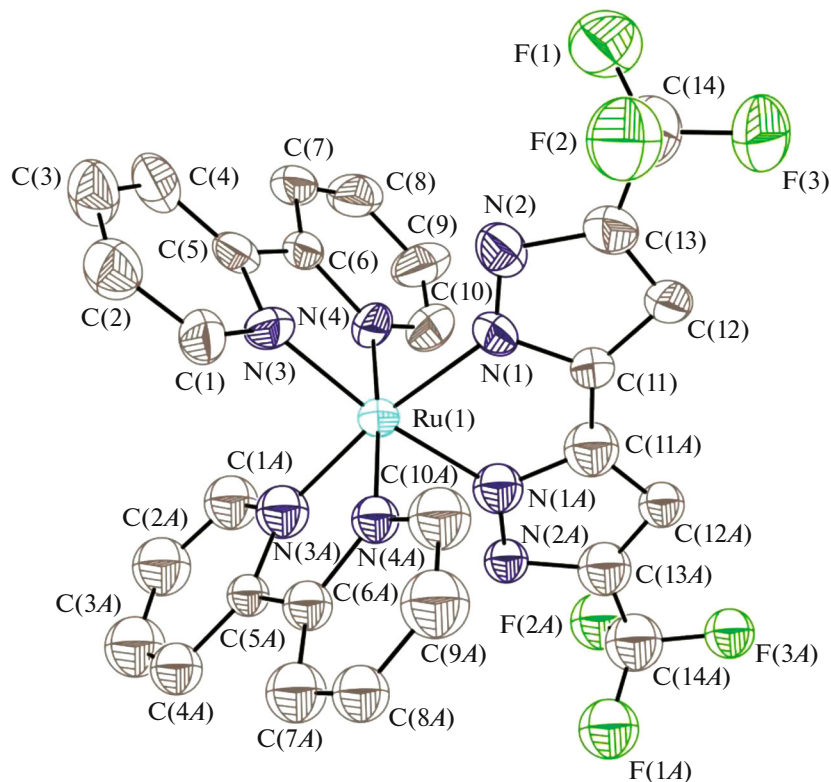


**Fig. 1.** Molecular structure of  $\mathbf{I} \cdot \text{H}_2\text{O}$ . Thermal ellipsoids are shown at the 40% probability level. The water molecule and hydrogen atoms were omitted for clarity. Selected bond lengths and angles:  $\text{Ru(1)}-\text{N(1)}$  2.063(12),  $\text{Ru(1)}-\text{N(3)}$  1.959(10),  $\text{Ru(1)}-\text{N(4)}$  2.016(11),  $\text{N(1)}-\text{N(2)}$  1.316(17),  $\text{N(1)}\text{Ru(1)}\text{N(1A)}$  79.6(6) Å and  $\text{N(3)}\text{Ru(1)}\text{N(4)}$  80.2(3)°,  $\text{N(1)}\text{Ru(1)}\text{N(3A)}$  171.0(4)°,  $\text{N(4)}\text{Ru(1)}\text{N(4A)}$  176.3(6)°. (A)  $y, x, -z + 1$ .

complexes have relatively good solubility in common organic solvents and are stable in solid for a relatively long time and also stable in solution for several months as deduced from spectroscopic studies.

Molecular structures of complexes  $\mathbf{I} \cdot \text{H}_2\text{O}$ ,  $\mathbf{III} \cdot \text{H}_2\text{O}$  and  $\mathbf{IV}$  have been established by X-ray crystallography. Structures of these neutral and cationic heteroleptic ruthenium(II)-Bipy/Dmbipy complexes are shown in Figs. 1–3. The central ruthenium atoms of three complexes are in an octahedral coordination environment, the ruthenium(II) complexes contain two Bipy or Dmbipy units and one bidentate Bipz<sup>2-</sup> or Pypz<sup>-</sup> ligand. The  $\text{Ru}-\text{N}(\text{Bipy}/\text{Dmbipy})$  bond lengths in  $\mathbf{I} \cdot \text{H}_2\text{O}$ ,  $\mathbf{III} \cdot \text{H}_2\text{O}$  and  $\mathbf{IV}$  range from 1.959(10) to 2.066(6) Å, which are slightly shorter than the  $\text{Ru}-\text{N}(\text{Py})$  bond lengths in  $\mathbf{III} \cdot \text{H}_2\text{O}$  and  $\mathbf{IV}$  (2.084(7)–2.087(6) Å). The  $\text{Ru}-\text{N}(\text{Pz})$  bond length of 2.063(12) Å in complex  $\mathbf{I} \cdot \text{H}_2\text{O}$  are a little longer than those in complexes  $\mathbf{III} \cdot \text{H}_2\text{O}$  (2.030(6) Å) and  $\mathbf{IV}$  (2.029(6) Å), possibly due to the existence of two electron-withdrawing trifluoromethyl substituents on Bipz<sup>2-</sup> ligand, which decreases the electron density of pyrazolate nitrogen. The similar  $\text{Ru}-\text{N}(\text{Pz})$  bond lengths in  $\mathbf{III} \cdot \text{H}_2\text{O}$  (2.030(6) Å) and  $\mathbf{IV}$  (2.029(6) Å) indicate the substituents of methyl groups on Bipy

units having little effect on the bond parameters of  $\text{Ru}-\text{N}(\text{Pz})$ . As expected, the  $\text{Ru}-\text{N}(\text{Pz})$  bond length gives the shortest  $\text{Ru}-\text{N}$  distances within the entire molecules of  $\mathbf{III} \cdot \text{H}_2\text{O}$  and  $\mathbf{IV}$  [14]. Meanwhile, a tendency for increased ruthenium–nitrogen bond lengths in the *trans* position with respect to the  $\text{Ru}-\text{N}(\text{Pz})$  bond is observed in  $\mathbf{III} \cdot \text{H}_2\text{O}$  (2.050(6) Å vs 2.032(7) Å) and  $\mathbf{IV}$  (2.065(6) Å vs 2.041(6) Å), which is identical with related  $[\text{Ru}(\text{Bipy})_2(\text{C}^{\text{N}})]^+$  complexes [22]. The chelate bond angles of  $\text{N}(\text{Py})\text{RuN}(\text{Pz})$  in  $\mathbf{III} \cdot \text{H}_2\text{O}$  and  $\mathbf{IV}$  are 78.7(3)° and 78.8(2)°, respectively, which are compared with few ruthenium(II) complexes with Pypz<sup>-</sup> ligand (77.5(6)°–78.0(4)°) [14, 25]. The  $\text{N}(\text{Pz})\text{RuN}(\text{Pz})$  bond angle in  $\mathbf{I} \cdot \text{H}_2\text{O}$  is 79.6(6)°, a little larger than those in iridium(III) and platinum(II) complexes with Bipz<sup>2-</sup> ligand (77.0(6)°–78.1(6)°) [26, 27]. Moreover, the three complexes have similar  $\text{N}(\text{Bipy})\text{RuN}(\text{Bipy})$  bond angles (78.5(2)°–78.8(2)°), a suggestive of the stable rigid structure of Bipy units.

Crystal packing in molecules  $\mathbf{I} \cdot \text{H}_2\text{O}$ ,  $\mathbf{III} \cdot \text{H}_2\text{O}$  and  $\mathbf{IV}$  are all governed by the weak intermolecular C–H···N hydrogen-bonding interactions (see Table 2). Besides, C–H···F hydrogen-bonding interactions between  $\text{PF}_6^-$  and  $[\text{Ru}(\text{Pypz})(\text{Bipy})_2]^+$  or  $[\text{Ru}(\text{Pypz})(\text{Dmbipy})_2]^+$  exist

**Table 2.** Geometric parameters of hydrogen-bond for complexes **I**·H<sub>2</sub>O, **III**·H<sub>2</sub>O, and **IV**\*

D—H···A	Distance, Å			∠(DHA, deg)
	D—H	H···A	D···A	
<b>I</b> ·H <sub>2</sub> O				
C(10)—H(10)···N(1) <sup>i</sup>	0.93	2.55	3.124(18)	120.0
<b>III</b> ·H <sub>2</sub> O				
C(24)—H(24)···F(5) <sup>ii</sup>	0.93	2.53	3.204(14)	130.0
C(10)—H(10)···N(7) <sup>iii</sup>	0.93	2.57	3.498(13)	175.9
C(13)—H(13)···N(7) <sup>iii</sup>	0.93	2.53	3.461(12)	176.6
C(8)—H(8)···N(1)	0.93	2.62	3.168(11)	118.1
C(15)—H(15)···N(6)	0.93	2.66	3.211(11)	118.5
<b>IV</b>				
C(10)—H(10)···F(4)	0.93	2.50	3.150(11)	126.8
C(31)—H(31)···N(1)	0.93	2.67	3.191(11)	116.0
C(22)—H(22)···N(5)	0.93	2.61	3.130(9)	116.2
C(5)—H(5)···N(7) <sup>iv</sup>	0.93	2.50	3.397(10)	162.9
C(28)—H(28)···F(1) <sup>v</sup>	0.93	2.61	3.530(11)	170.7

\* Symmetry codes: <sup>i</sup>  $y, x, -z + 1$ ; <sup>ii</sup>  $x + 1, y, z$ ; <sup>iii</sup>  $-x + 2, -y + 1, -z + 2$ ; <sup>iv</sup>  $-x, -y, -z + 2$ ; <sup>v</sup>  $-x + 1/2, y + 1/2, -z + 3/2$ .

in cationic complexes **III**·H<sub>2</sub>O and **IV**. The separations of H···N in the three molecules are in the range of 2.50–2.67 Å, similar to the H···F distances in complexes **III**·H<sub>2</sub>O (2.53 Å) and **IV** (2.50, 2.61 Å). The hydrogen-bond angles of C—H···N are 120.0° for complex **I**·2H<sub>2</sub>O, 118.3° and 176.0° for complex **III**·H<sub>2</sub>O, together with 116.1° and 162.9° for complex **IV**. Moreover, the C—H···F bond angles are 130.0° in complex **III**·H<sub>2</sub>O, 126.8° and 170.7° in molecule of complex **IV**. Such rich hydrogen-bond interactions of C—H···N and C—H···F all contribute to the stabilization of the three crystal structures.

The UV-Vis absorption spectra of new heteroleptic ruthenium(II) complexes **I**–**IV**, together with the parent complex [Ru(Bipy)<sub>3</sub>](PF<sub>6</sub>)<sub>2</sub>, in CH<sub>2</sub>Cl<sub>2</sub> at room temperature are shown in Fig. 4. At the first glance, spectra for complexes **I**–**IV** are grossly similar and reveal three intense transitions located at 240–280, 340–390 and 470–550 nm. The strong absorption bands around 260 nm are assigned to a typical spin-allowed  $^1\pi-\pi^*$  transition of the ligands, and the comparatively less intense broad bands around 370 and 530 nm are ascribed to the metal-to-ligand charge transfer (MLCT) transitions. These spectra are similar to that of [Ru(Bipy)<sub>3</sub>](PF<sub>6</sub>)<sub>2</sub> and related ruthenium(II)-Bipy complexes with additional *N,N*- or *N,O*-donors [11, 16, 17]. For example, ruthenium Bipy/Bipz<sup>2+</sup> derivative with the 2,2'-Bipy ligand substituted by two carboxylates showed three absorption bands at around 308, 391 and 547 nm [11]. Cationic

complexes **III** and **IV** with Pypz<sup>–</sup> ligands, which bear one electron-withdrawing –CF<sub>3</sub> group, have identical UV-Vis absorption properties. The difference of low-lying MLCT bands in the spectra of **I** and **II** with Bipz<sup>2+</sup> ligands bearing two electron-withdrawing –CF<sub>3</sub> groups, possibly arises from the existence of four methyl substituents on two Bipy units, which affords a more electron-rich ruthenium center in complex **II** than that in complex **I**. It is interesting to note that there is a red-shift of about 50 nm observed for the low-lying transition depending on the presence of coordination of the Bipz<sup>2+</sup> and Pypz<sup>–</sup> ligands. This considerable shift suggests that the low-energy transition is the main signature of the charge transfer arising between the ruthenium atom and Bipy or Dmbipy ligand [28].

The room temperature photoluminescence spectra of the heteroleptic ruthenium(II) complexes **I**–**IV** and [Ru(Bipy)<sub>3</sub>](PF<sub>6</sub>)<sub>2</sub> in CH<sub>2</sub>Cl<sub>2</sub> solution are illustrated in Fig. 5. These neutral and cationic ruthenium(II) complexes show similar orange emission due to their structural similarity. But there are still faint differences among them. Complexes **I**–**IV** all emit weak luminescence with emission wavelengths at 644, 651, 632, and 655 nm, respectively, red shifted compared to that of [Ru(Bipy)<sub>3</sub>](PF<sub>6</sub>)<sub>2</sub> (598 nm). This result possibly reflects the better electron-donor ability of anionic auxiliary ligands of bipyrazolate and 2-pyridylpyrazolate than the neutral Bipy donor [16]. Complexes **II**

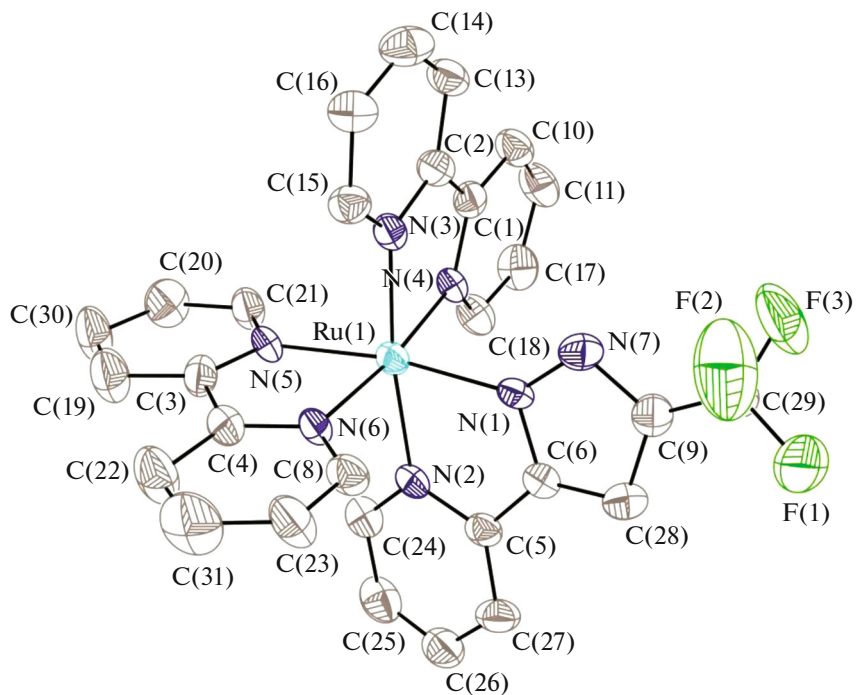


**Fig. 2.** Molecular structure of cationic  $[\text{Ru}(\text{Pypz})(\text{Bipy})_2]^+$  in **III**· $\text{H}_2\text{O}$ . Thermal ellipsoids are shown at the 40% probability level. The counter anion and hydrogen atoms were omitted for clarity. Selected bond lengths and angles:  $\text{Ru}(1)-\text{N}(1)$  2.030(6),  $\text{Ru}(1)-\text{N}(2)$  2.084(7),  $\text{Ru}(1)-\text{N}(3)$  2.032(7),  $\text{Ru}(1)-\text{N}(4)$  2.036(7),  $\text{Ru}(1)-\text{N}(5)$  2.050(6),  $\text{Ru}(1)-\text{N}(6)$  2.061(6),  $\text{N}(1)-\text{N}(7)$  1.327(9) Å and  $\text{N}(1)\text{Ru}(1)\text{N}(2)$  78.7(3)°,  $\text{N}(3)\text{Ru}(1)\text{N}(4)$  78.5(3)°,  $\text{N}(5)\text{Ru}(1)\text{N}(6)$  78.5(2)°,  $\text{N}(1)\text{Ru}(1)\text{N}(5)$  170.7(2)°,  $\text{N}(2)\text{Ru}(1)\text{N}(3)$  172.4(2)°,  $\text{N}(4)\text{Ru}(1)\text{N}(6)$  173.4(3)°.

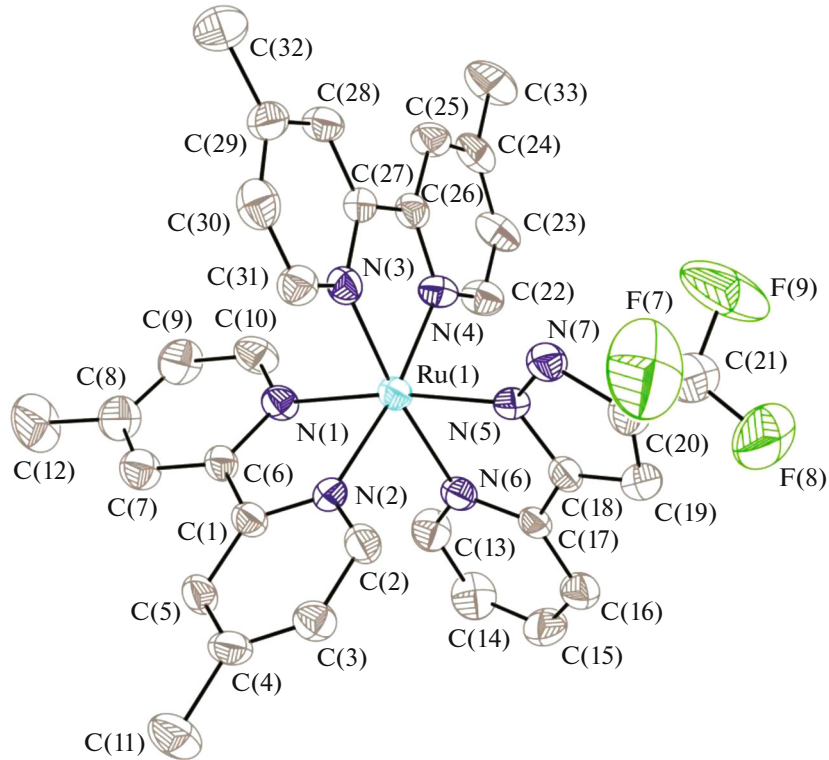


**Fig. 3.** Molecular structure of cationic  $[\text{Ru}(\text{Pypz})(\text{Dmbipy})_2]^+$  in **IV**. Thermal ellipsoids are shown at the 40% probability level. The counter anion and hydrogen atoms were omitted for clarity. Selected bond lengths and angles:  $\text{Ru}(1)-\text{N}(1)$  2.052(6),  $\text{Ru}(1)-\text{N}(2)$  2.041(6),  $\text{Ru}(1)-\text{N}(3)$  2.065(6),  $\text{Ru}(1)-\text{N}(4)$  2.056(6),  $\text{Ru}(1)-\text{N}(5)$  2.029(6),  $\text{Ru}(1)-\text{N}(6)$  2.087(6),  $\text{N}(5)-\text{N}(7)$  1.348(7) Å and  $\text{N}(1)\text{Ru}(1)\text{N}(2)$  78.6(2)°,  $\text{N}(3)\text{Ru}(1)\text{N}(4)$  78.8(2)°,  $\text{N}(5)\text{Ru}(1)\text{N}(6)$  78.8(2)°,  $\text{N}(1)\text{Ru}(1)\text{N}(5)$  171.5(2)°,  $\text{N}(2)\text{Ru}(1)\text{N}(4)$  171.6(2)°,  $\text{N}(3)\text{Ru}(1)\text{N}(6)$  173.1(2)°.

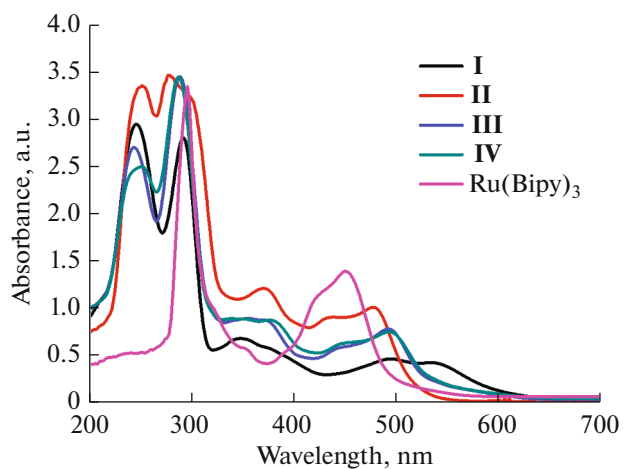


Fig. 4. The UV-Vis absorption spectra of complexes I–IV and  $[\text{Ru}(\text{Bipy})_3](\text{PF}_6)_2$  in  $\text{CH}_2\text{Cl}_2$  solution.

and **IV** with Me-Bipy units are red shifted compared to their corresponding H-Bipy analogues **I** and **III** (651 vs. 644 nm; 655 vs. 632 nm) since methyl substituents are electron-donating groups [29].

In summary, four new heteroleptic ruthenium(II)-Bipy/Dmbipy complexes incorporating bipyrazolate and 2-pyridyl pyrazolate ancillaries were synthesized by reaction of *cis*- $[\text{RuCl}_2(\text{Bipy})_2]\cdot 2\text{H}_2\text{O}$  or *cis*- $[\text{RuCl}_2(\text{Dmbipy})_2]\cdot 2\text{H}_2\text{O}$  with BipzH<sub>2</sub> and/or PypzH ligand in moderate yields. According to a CCDC search, only iridium and platinum complexes with bipyrazolate ligands were available [26, 27], isolation of the two bipyrazolate-based ruthenium(II) complexes confirm that bipyrazolate could also coordinate to ruthenium(II) [11]. Meanwhile, the two new complexes with 2-pyridyl pyrazolate ligands enriched the structures of limited Pypz-based ruthenium com-

plexes [14, 25]. An X-ray study highlighted the specific features of the Ru–N(Pz) and the *trans*-Ru–N(Py) bonds for Pypz-based ruthenium complexes **III**·H<sub>2</sub>O and **IV**. The three structures may be probably stabilized by C–H···N and C–H···F hydrogen-bonding interactions. An enhanced MLCT effect occurred in the presented heteroleptic ruthenium(II) complexes compared to the parent  $[\text{Ru}(\text{Py})_3](\text{PF}_6)_2$  molecule. This information is of interest and importance for the design and synthesis of a new heteroleptic ruthenium(II)–Bipy system.

#### FUNDING

This project was supported by the Natural Science Foundation of China (21372007).

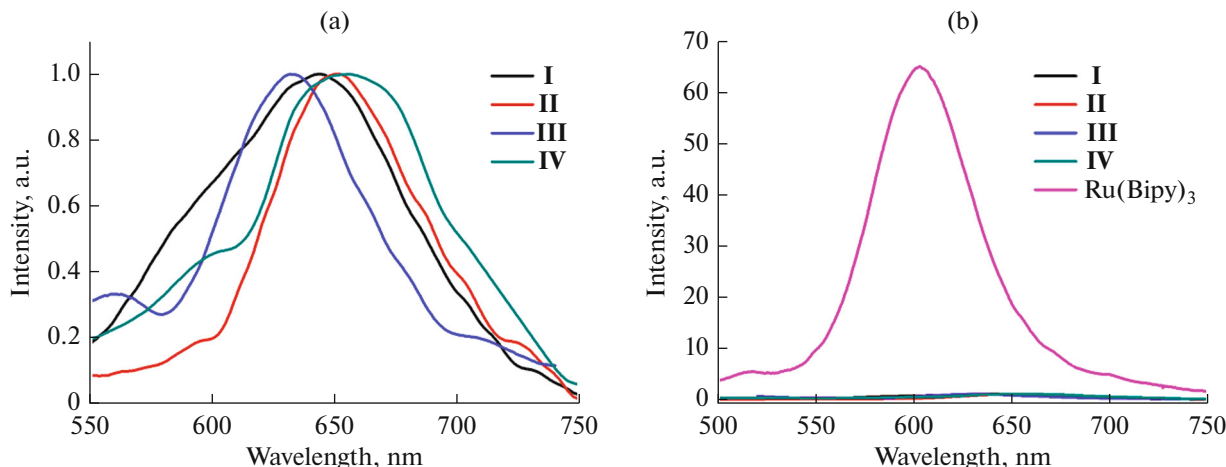


Fig. 5. Photoluminescence spectra of complexes I–IV (a) and  $[\text{Ru}(\text{Bipy})_3](\text{PF}_6)_2$  (b) in  $\text{CH}_2\text{Cl}_2$  solution.

## REFERENCES

- Norris, M.R., Concepcion, J.J., Harrison, D.P., et al., *J. Am. Chem. Soc.*, 2013, vol. 135, no. 6, p. 2080.
- Stumper, A., Pilz, T.D., Schaub, M., et al., *Eur. J. Inorg. Chem.*, 2017, vol. 2017, no. 32, p. 3799.
- Raden, J.F.V., Louie, S., Zakharov, L.N., et al., *J. Am. Chem. Soc.*, 2017, vol. 139, no. 8, p. 2936.
- Kundu, T., Chowdhury, A.D., De, D., et al., *Dalton Trans.*, 2012, no. 41, p. 4484.
- Zhang, W., Liu, J.-H., Pan, J.-X., et al., *Polyhedron*, 2008, vol. 27, no. 4, p. 1168.
- Mulhern, D., Brooker, S., Görls, H., et al., *Dalton Trans.*, 2006, no. 1, p. 51.
- Naskar, S., Pakhira, B., Mishra, D., et al., *Polyhedron*, 2015, vol. 100, p. 170.
- Liao, J.-L., Chi, Y., Liu, S.-H., et al., *Inorg. Chem.*, 2014, vol. 53, no. 17, p. 9366.
- Liao, J.-L., Chi, Y., Yeh, C.-C., et al., *J. Mater. Chem. C*, 2015, vol. 3, no. 19, p. 4910.
- Hsu, C.-W., Zhao, Y.-B., Yeh, H.-H., et al., *J. Mater. Chem. C*, 2015, vol. 3, no. 41, p. 10837.
- Yeh, H.-H., Ho, S.-T., Chi, Y., et al., *J. Mater. Chem. A*, 2013, vol. 1, no. 26, p. 7681.
- Liao, J.-L., Chi, Y., Sie, Z.-T., et al., *Inorg. Chem.*, 2015, vol. 54, no. 22, p. 10811.
- Chen, K., Hong, Y.-H., Chi, Y., et al., *J. Mater. Chem.*, 2009, vol. 19, no. 30, p. 5329.
- Chen, B.-S. and Chen, K., Hong, Y.-H., et al., *Chem. Commun.*, 2009, no. 39, p. 5844.
- Chou, C.-C., Hu, F.-C., Wu, K.-L., et al., *Inorg. Chem.*, 2014, vol. 53, no. 16, p. 8593.
- Wang, Z.-M., Shen, S.-M., Shen, X.-Y., et al., *J. Coord. Chem.*, 2016, vol. 69, no. 5, p. 851.
- Wang, C.-J., Xu, W.-F., Tong, B.-H., et al., *J. Coord. Chem.*, 2017, vol. 70, no. 10, p. 1617.
- Ji, J., Li, G.-Q., Xu, Y.-Q., et al., *Z. Naturforsch., B: Chem. Sci.*, 2019, vol. 74b, p. 267.
- Sullivan, B.P. and Salmon, D.J., *Inorg. Chem.*, 1978, vol. 17, no. 12, p. 3334.
- Seok, W.K., Jo, M.R., Kim, N., et al., *Z. Anorg. Allg. Chem.*, 2012, vol. 638, no. 5, p. 754.
- Lay, P.A., Sargeson, A.M., Taube, H., et al., *Inorg. Synth.*, 2007, vol. 291, p. 45.
- SMART and SAINT+ for Windows NT Version 6.02a*, Madison: Bruker Analytical X-ray Instruments Inc., 1998.
- Sheldrick, G.M., *SADABS*, Göttingen: Univ. of Göttingen, 1996.
- Sheldrick, G.M., *SHELXTL, Software Reference Manual*, Version 5.1, Madison: Bruker AXS Inc., 1997.
- Wu, P.-C., Yu, J.-K., Song, Y.-H., et al., *Organometallics*, 2003, vol. 22, no. 24, p. 4938.
- Li, Y.-S., Liao, J.-L., Lin, K.-T., et al., *Inorg. Chem.*, 2017, vol. 56, no. 16, p. 10054.
- Liao, J.-L., Chi, Y., Wang, J.-Y., et al., *Inorg. Chem.*, 2016, vol. 55, no. 13, p. 6394.
- Labat, L., Lamere, J.-F., Sasaki, I., et al., *Eur. J. Inorg. Chem.*, 2006, vol. 2006, no. 15, p. 3105.
- Zhang, M., Hu, Y.-Y., Pan, M., et al., *Dyes Pigments*, 2019, vol. 165, p. 11.